Bull. Mater. Sci., Vol. 40, No. 4, August 2017, pp. 791–797
DOI 10.1007/s12034-017-1404-2

Interplay of the influence of oxygen partial pressure and rf power on the properties of rf-magnetron-sputtered AZO thin films

A KASSIS*, M SAAD and F NOUNOU
Atomic Energy Commission of Syria, P.O. Box 6091, Damascus, Syria
*Author for correspondence (pscientific2@aec.org.sy)

MS received 14 June 2016; accepted 17 August 2016; published online 25 July 2017

Abstract. The complex interplay between the influence of oxygen partial pressure and that of rf power on the structural, electrical and optical properties of rf-magnetron-sputtered aluminium-doped zinc oxide, AZO, thin films is illustrated. The dependence of film electrical resistance and interplanar spacing of film crystallites on rf power seems to be different at higher oxygen partial pressure values than at lower ones. Film preparation was performed at room temperature (without extra heating) and low pressure $p = 0.5$ mTorr, varying the rf power density between $P = 0.57$ and 2.83 W cm^{-2} at different relative oxygen partial pressure values. An explanation of film properties has been sought in terms of changes in the chemical properties of the films due to the bombardment of the films during film formation with negative oxygen ions.

Keywords. Sputtering; oxides; thin films; electrical resistance; optical properties; X-ray photo-emission spectroscopy.

1. Introduction

Zinc oxide (ZnO) and aluminium-doped zinc oxide (AZO) thin films are used as window layers in solar cells [1–3]. Sputtering (especially rf magnetron sputtering [4]) is one of the most common choices for depositing these films due to its high deposition rate and the high stability of the films. ZnO, the basis material for AZO, is naturally an n-type semiconductor due to its deviation from stoichiometry and hence to the presence of oxygen vacancies or zinc interstitials [5,6]. Addition of oxygen during deposition is expected to affect film properties, such as crystallinity [7,8], optical band gap and carrier concentrations [9]. It is reasonably expected that oxygen vacancies would decrease with the addition of oxygen to the argon sputtering gas; however, atomic O/Zn ratios larger than 1 in the deposited films have been reported for ZnO films prepared with addition of oxygen to the sputtering gas at various rf power and total pressure values as well as oxygen partial pressure values [10]. In addition to influencing the oxygen vacancies, adding oxygen to the sputtering gas provides the plasma with an extra portion of negative ions and leads to increased bombardment of the film with high-energy ions during film growth. This would generally lead to a higher defect density [11,12].

In the literature there are works reporting the effect of rf power on certain properties of ZnO or AZO thin films [13–15] and others reporting the effect of oxygen addition to the sputtering gas [16,17]. One can also find some works studying the effect of both rf power and oxygen addition on some aspects of film properties [10,18–20]. However, as far as we know, there is no work so far studying the interplay between the influence of rf power and that of oxygen addition to the sputtering gas on the properties of AZO thin films.

In our previous work [13] that studied the effect of rf power on the properties of rf-magnetron-sputtered AZO thin films, film resistance was found to be much more correlated with the interplanar spacing within the crystallites than with film crystallite size. This correlation was explained through the number of Al atoms occupying interstitial places, which seems to increase with rf power, leading to larger interplanar spacing and higher electrical resistance.

In this study we shed light on the interplay between the influences of two important deposition parameters on the properties of rf-magnetron-sputtered AZO films: rf power density (P) and oxygen partial pressure (OPP) in the sputtering gas. For this purpose a set of films prepared under different conditions and carefully selected deposition parameters is studied and the results are discussed. The films were deposited at room temperature (without substrate heating) and low pressure of $p = 0.5$ mTorr. The relative OPP varied between $OPP = 0$ and 6%, and the rf power density between $P = 0.57$ and 2.83 W cm^{-2}. The structural, electrical and optical properties of the films are analysed and discussed.

2. Experimental

AZO films are deposited using an rf magnetron sputtering system (Plassys MP 600S). Target diameter is 150 mm and target-to-substrate distance is fixed at 50 mm. Target composition is ZnO + 2 wt% Al_2O_3 (99.99% purity). The rf power is supplied by a 13.56 MHz 1 kW rf generator (Cesar 1310,

Dressler Hochfrequenztechnik GmbH). Glass substrates are ultrasonically cleaned using methanol and de-ionized water, and then dried in nitrogen atmosphere. During deposition, the total argon–oxygen gas pressure was adjusted to be $p = 0.5$ mTorr. Relative *OPP* is set to one of the following values: $OPP = 0$, 3 or 6%, by adjusting the argon and oxygen flow rates. Rf power density is varied between $P = 0.57$ and 2.83 W cm^{-2}, with deposition rates varying accordingly between 0.1 and 1.2 nm s^{-1} (see figure 1). Film thickness is nominally set to $t = 100$ nm with the help of a thickness monitor. Depositions are performed at room temperature (without extra heating).

To analyse the crystalline structure and orientation of the AZO films, an X-ray diffractometer (STOE STADI P) is used with Cu K_α radiation filtered by a crystal monochromator ($\lambda = 0.15417$ nm). The X-ray source is operated at 50 kV and 30 mA. Furthermore, a SPECS UHV/XPS/AES system with a hemispherical energy analyser was used for X-ray photoemission spectroscopy (XPS) investigation.

Optical transmission measurements are accomplished with a spectrophotometer (Photodiode array Stecord S100, Analytik Jena) between 300 and 1000 nm using bare glass as a reference sample. Electrical resistance is obtained from the current–voltage curve of each AZO film at room temperature using a Keithley 238 Source Measure Unit.

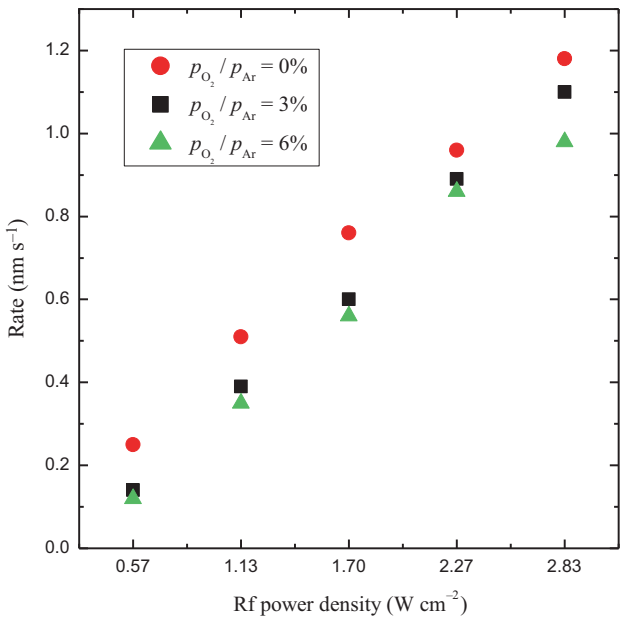

Figure 1. Deposition rate as a function of rf power density P at different values of oxygen partial pressure, *OPP*.

3. Results and discussion

3.1 *Structural properties*

Figure 1 shows the dependence of deposition rate on both rf power density P and *OPP*. As can be seen, P is the main factor influencing deposition rate, whereas the influence of *OPP* on that rate is less dominant. Deposition rate increases linearly with P, and decreases slightly with increasing *OPP* due to resputtering by the negative oxygen ions [12]. Deposition rate interplays with the sputtered particle energy in a complex way that leads to a tradeoff between small deposition rate and high particle energy to form a good crystalline thin film with a stoichiometric composition, as stated in an earlier work [13]. Adding oxygen to the sputtering gas did not change the deposition rate much, but did affect the AZO film properties very much. The influence of *OPP* on the structure of AZO thin films was investigated using X-ray diffraction (XRD). Figure 2 compares XRD measurements on thin films grown at different rf power density values, each for different *OPP* in the working gas. The films have hexagonal wurtzite structure. A prominent (002) peak was observed regardless of the *OPP*, indicating a crystallite growth with the *c*-axis perpendicular to the substrate [21]. This figure shows XRD measurements on AZO thin films deposited at different rf power density

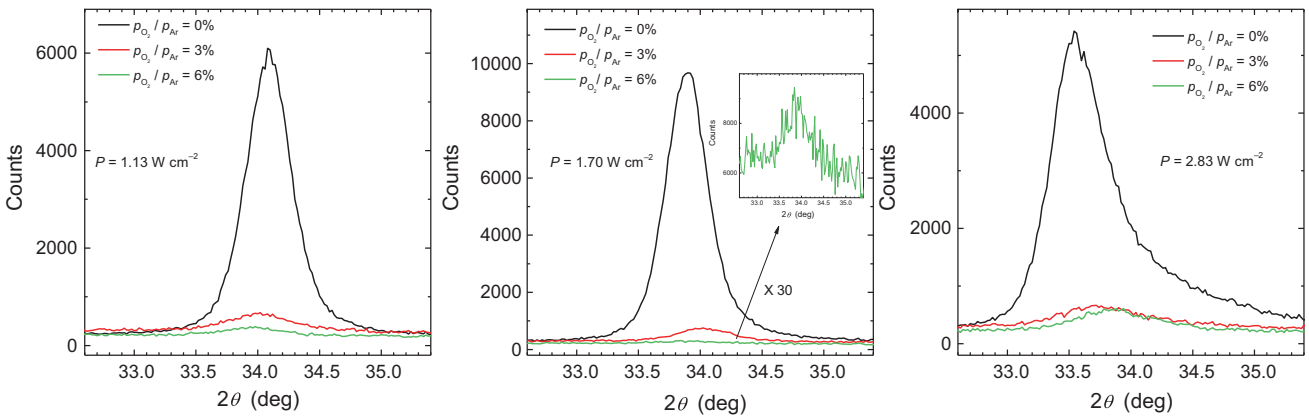

Figure 2. X-ray diffraction measurements on AZO thin films grown at different rf power density values P and different values of oxygen partial pressure, *OPP*.

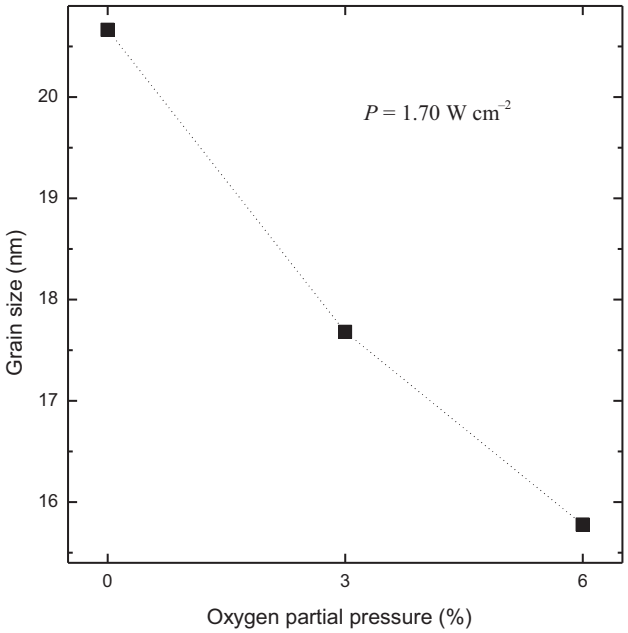

Figure 3. Dependence of mean crystallite size D of the deposited AZO thin films at $P = 1.70$ W cm^{-2} on oxygen partial pressure, *OPP*.

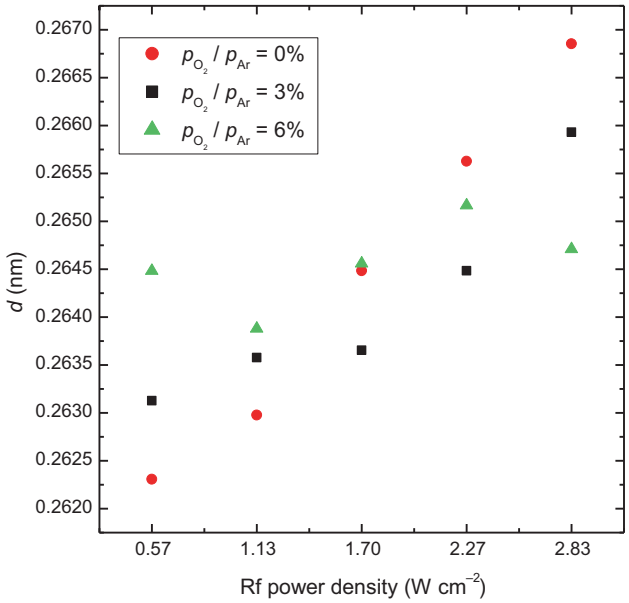

Figure 4. Dependence of calculated d-spacing values for the deposited AZO thin films on rf power density P for different values of oxygen partial pressure, *OPP*.

values and different values of *OPP*. As *OPP* was increased, the peak intensity decreased for all rf power density values and the peak became more broadened. This figure also shows that high *OPP* leads to a deterioration of crystallite growth for all rf power density values.

The mean crystallite size D of the films can be calculated using Scherrer's formula with a shape factor value of $k = 0.94$ [22]. Figure 3 shows the dependence of these calculated values on *OPP* at rf power density $P = 1.70\,\mathrm{W\,cm^{-2}}$. As *OPP* was increased, the crystalline quality of the films deteriorated and the grain size decreased from 20.7 to 15.8 nm.

From the XRD measurements not only the mean crystallite size D but also the interplanar spacing between the X-ray reflecting planes, the so-called d-spacing, can be calculated using the Bragg diffraction formula $\lambda = 2d \sin\theta$. Figure 4 shows the dependence of calculated d-spacing values for the deposited AZO thin films on rf power density for different *OPP* values. It can be seen that with increasing *OPP* the dependence of d-spacing on rf power density becomes weaker. It seems that oxygen ion bombardment onto the thin film being formed and increasing rf power density generally increase the portion of interstitial atoms of all species, leading to an increase in the d-spacing in the AZO crystallites. At higher rf power density and with the presence of excess oxygen ions in the plasma, the higher energy of sputtered particles and the slightly lower deposition rate seem to favour the formation of more stoichiometric ZnO crystallites, whereas the Al atoms seem to be bonded with oxygen to form Al_2O_3 at grain boundaries. This may explain the decrease in the d-spacing at elevated *OPP* and at the same time at high rf power density.

For more insight on the energetic states of the chemical compounds of the films, XPS measurements have been performed, and their results are presented.

The binding energy of oxygen, zinc and aluminium in the deposited films was measured using XPS. Figure 5 compares the O 1s core peak for different *OPP* values (*OPP* = 0, 3 and 6%) at three different rf power density values ($P = 1.13$, 1.70 and 2.83 W cm^{-2}). Figure 6 shows the same comparison for the Zn $2p_{3/2}$ core peak. The O 1s peak has been deconvoluted into two peaks, a low energy one at about 530.3 eV (related to the O–Zn bond in the wurzite structure [23]), and a higher energy one at about 531.8 eV (related to oxygen bonds with several species like $-$OH, $-CO_3$ and adsorbed H_2O or O_2 at film surface and grain boundaries [24]). It is clear from figure 5 that the second peak shifts to still higher energies with increasing *OPP* for all rf power density values. Furthermore, at rf power density $P = 1.13\,\mathrm{W\,cm^{-2}}$, the higher energy peak becomes stronger with increasing *OPP* (an indication of an increase in higher energy bonds relative to O–Zn ones); however, at rf power density $P = 2.83\,\mathrm{W\,cm^{-2}}$ the higher energy peak becomes weaker with increasing *OPP* (an indication of a decrease in higher energy bonds relative to O–Zn ones).

The Zn $2p_{3/2}$ peak seems to be symmetrical for all films. Its position is at about 1021.7 eV, which is between the energy of metallic Zn at 1021.5 eV (as an interstitial Zn atom in the lattice of ZnO) and the energy of Zn in Al-doped ZnO at 1021.9 eV [25] or at 1022.2 eV [26]; this Zn peak position seems also to be constant for rf power density $P = 1.13\,\mathrm{W\,cm^{-2}}$; however, for rf power density $P = 2.83\,\mathrm{W\,cm^{-2}}$ the peak position shifts to higher values with increasing *OPP* and takes a value

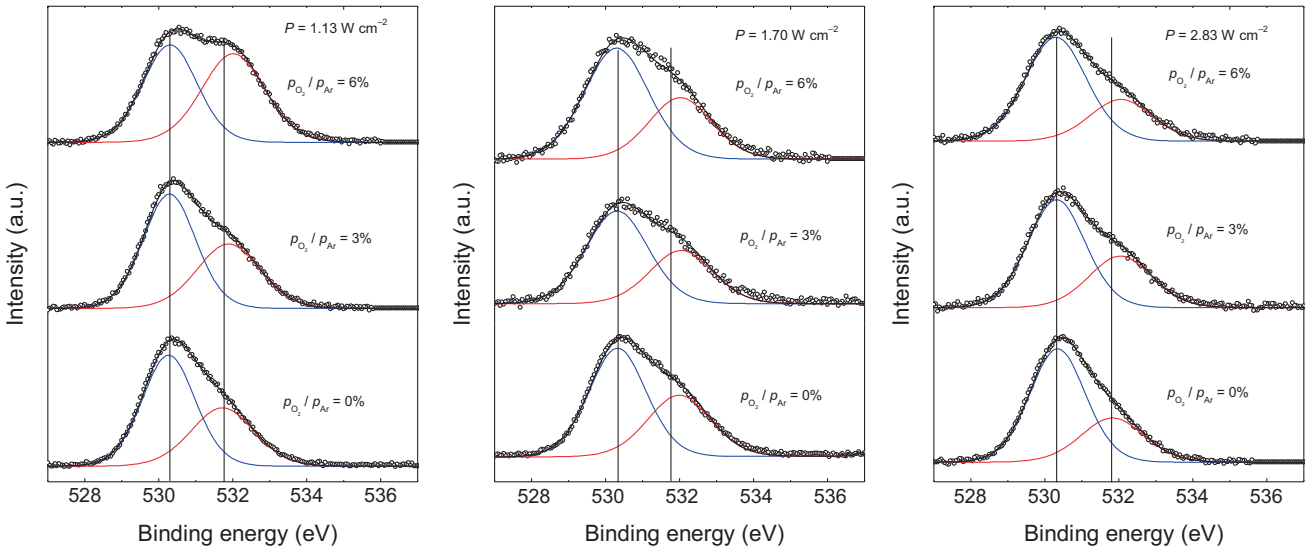

Figure 5. The O 1*s* core peak for different oxygen partial pressure values (*OPP* = 0, 3 and 6%) at three different rf power density values ($P = 1.13$, 1.70 and 2.83 W cm^{-2}). All peaks have been deconvoluted into two components. Two lines are drawn at 530.3 and 531.8 eV for guidance.

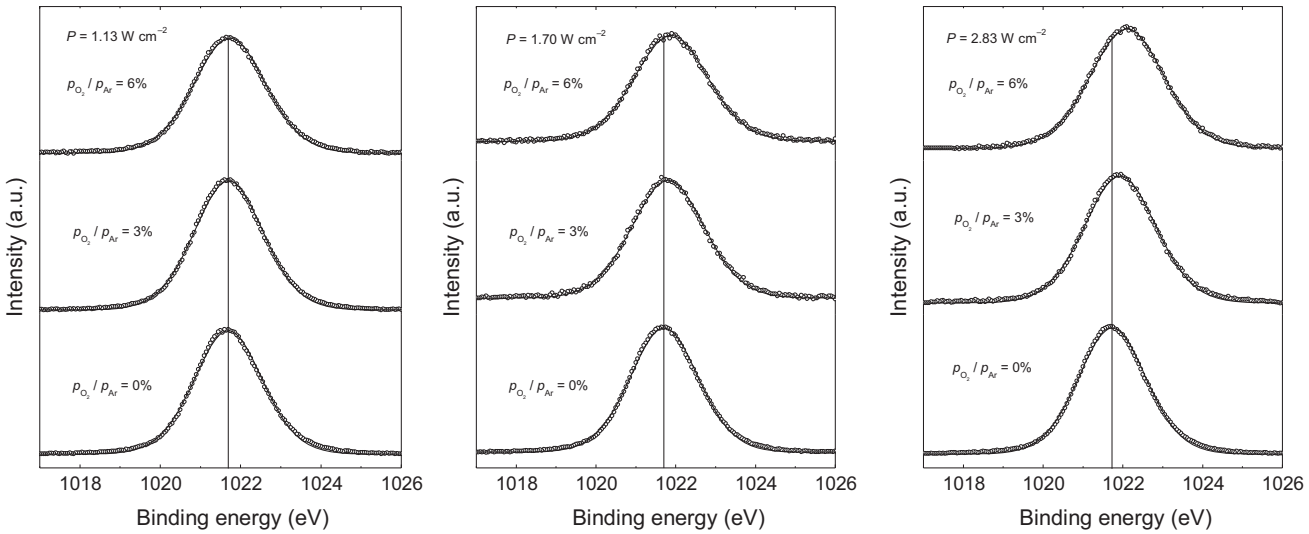

Figure 6. The Zn $2p_{3/2}$ core peak for different oxygen partial pressure values (*OPP* = 0, 3 and 6%) at three different rf power density values ($P = 1.13$, 1.70 and 2.83 W cm^{-2}).

near 1022.1 eV, corresponding to the Zn in the oxidized state Zn–O [27]. We can conclude that at higher rf power density values, the portion of metallic Zn decreases with increasing *OPP*, whereas that portion remains constant for low rf power density. This result supports the aforementioned argument that at higher rf power density values the higher *OPP* may favour the formation of a more stoichiometric ZnO, leading in turn to a decrease in the *d*-spacing values.

Furthermore, it should be mentioned that the spectra of the films prepared at high *OPP* values and at the same time at high rf power density values also exhibited a small Al peak at about 74 eV (not shown here), relatively near to the energy of Al in Al_2O_3 at 74.6 eV [26]. This fact also supports the aforementioned argument that at higher rf power density, the higher *OPP* may favour the formation of Al_2O_3 at the grain boundaries of ZnO crystallites, leading in turn to a decrease in the *d*-spacing values.

3.2 *Electrical properties*

Figure 7 shows a plot of log *R* *vs.* rf power density for AZO films deposited at various *OPP* values. Without oxygen addition the resistance *R* increases with increasing rf power density *P*. Such an increase has been related to an

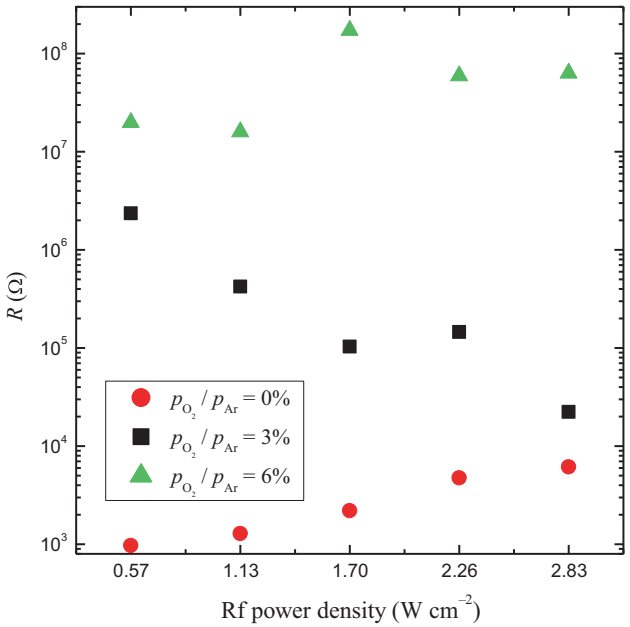

Figure 7. Dependence of log R on rf power density for AZO thin films prepared at different oxygen partial pressure values, *OPP*.

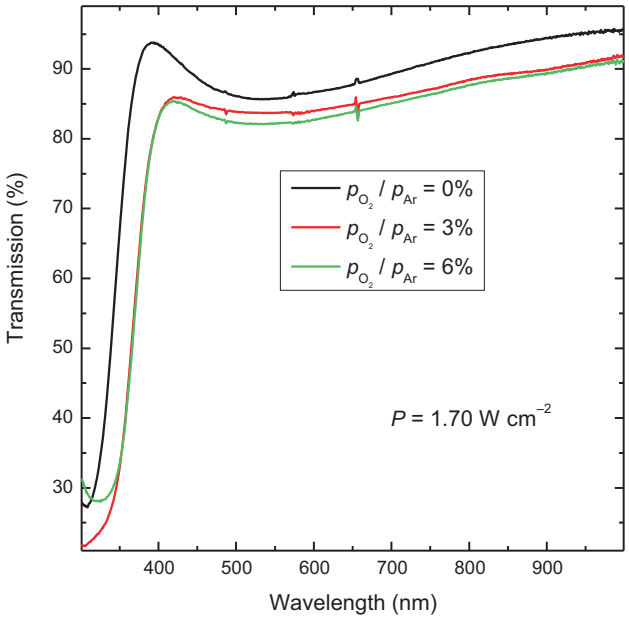

Figure 8. Optical transmission spectra of AZO thin films grown at rf power density of $P = 1.70$ W cm^{-2} with different oxygen partial pressure values, *OPP*.

increase in Al atoms occupying interstitial places and an increase in Al atoms occupying regular Zn ones [13]. A similar increase has been also reported by [28], while in another work R has been found to decrease with increasing P [29]; other groups found a non-monotonic dependence of R on P [30,31].

Figure 7 demonstrates a very different and remarkable behaviour of film resistance with increasing rf power density at various *OPP*. While R increases with increasing P for films deposited without additional oxygen, it seems obviously to decrease with increasing P for films deposited at an *OPP* of 3%; however, it seems to have very high values with no monotonic dependence on P for films deposited at an *OPP* value of 6%.

In a previous work [13] the behaviour of R depending on P for films deposited without oxygen addition has been explained in terms of the ratio of Al atoms occupying regular Zn places in the ZnO matrix to those occupying interstitial places. It has been stated there that this ratio decreased with increasing P, leading to increasing R. This explanation has been also used to explain the increase of d-spacing with increasing P. Here, this proposition will be developed further to explain the R behaviour for higher *OPP* values. As can be seen in figure 7, the addition of oxygen to the sputtering gas (in both cases of *OPP* = 3 and 6%) increases the film resistance drastically. This increase has been studied in relation with the suppression of oxygen vacancy defects [32] and with the bombardment of highly energetic oxygen species during sputtering [33] and the formation of Zn vacancy acceptors or the formation of homologous phases like $ZnAl_xO_y$ or Al_2O_3 in the AZO films [16,34–36]. Furthermore, it is well known that with the increment of *OPP* the Zn vacancies, oxygen interstitials and anti-site oxygen in ZnO will increase [16]. For the case of *OPP* = 3%, figure 7 shows that increasing the rf power density reduces the resistance. This could be related to a decrease in Zn vacancies, which favours formation of more stoichiometric ZnO crystallites due to the higher kinetic energy and thus higher diffusivity and ability to occupy the energetically lowest position. This in turn leads to a reduction of R without decreasing the d-spacing (although R is still high relative to that of AZO prepared without oxygen addition). In the case of *OPP* = 6% this mechanism seems to be ineffective in reducing R and it seems that the damage caused by the bombardment of negative ion oxygen species cannot be healed by the higher energy of sputtered particles.

3.3 *Optical properties*

Figure 8 compares optical transmission spectra on AZO thin films grown at rf power density of $P = 1.70$ W cm^{-2} with different *OPP* values. The transmission decreases with increasing *OPP* in the whole spectral range between 350 and 1000 nm. This can be related to a deterioration in film crystalline quality concerning crystallite size and concentration of various defects at grain boundaries as mentioned earlier, which in turn leads to more optical scattering and absorption. However, increasing *OPP* at higher P has led to more stoichiometric crystallites (as concluded from XRD and XPS measurements), a fact that would lead to a better optical transmission of the films; the negative effect of decreasing crystallite size with increasing *OPP* seems

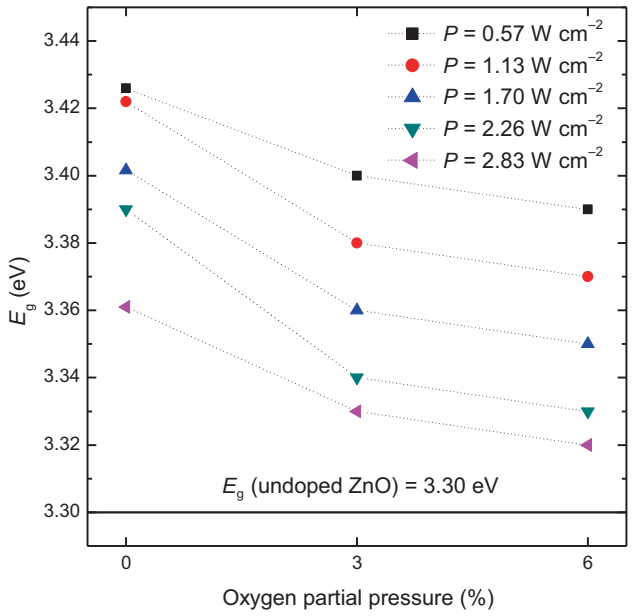

Figure 9. Dependence of obtained band gap values for AZO films prepared at different rf power densities on *OPP*.

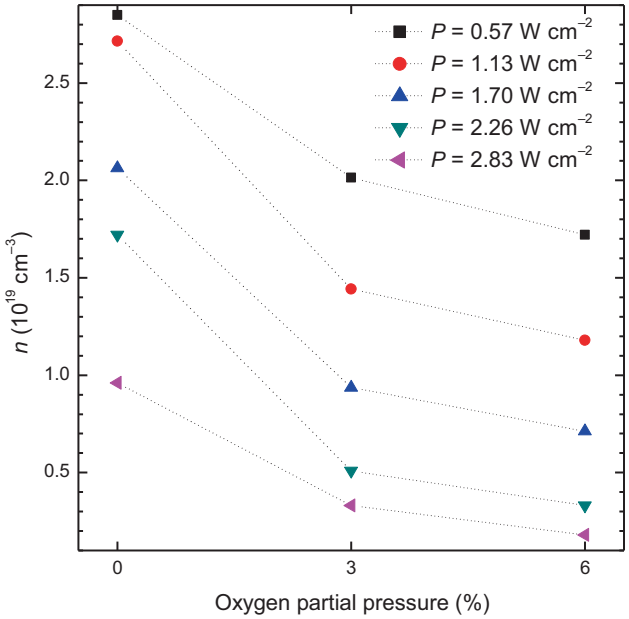

Figure 10. Dependence of calculated carrier concentration n of the studied AZO films prepared at different rf power densities on *OPP*.

to overweigh the positive effect of enhancing crystallite stoichiometry.

A Tauc plot of $(-\ln(T)h\upsilon)^2\ vs.\ h\upsilon$ [37], where T is the optical transmission and $h\upsilon$ is the photon energy, allows estimation of the optical band gap E_g of each film. The obtained band gap values for the films against different *OPP* values are presented in figure 9 for various rf power densities. The band gap values vary between 3.32 and 3.43 eV and decrease with increasing relative *OPP*. They are all larger than that of undoped bulk ZnO ($E_{g0} \approx 3.3$ eV [38]) due to the Burstein–Moss blue-shift [39–42].

From the band gap widening ΔE_g (the difference between the band gap of AZO and that of bulk ZnO), the carrier concentration n of the Al-doped films can be estimated with the help of the following equation [37]:

$$\Delta E_g = \left(\frac{h^2}{8m^*}\right)\left(\frac{3n}{\pi}\right)^{2/3}, \qquad (1)$$

where m^* is the electron effective mass in the conduction band ($m^* = 0.27\,m_0$ [33]). Figure 10 shows the calculated carrier concentration n of the studied films prepared at different relative *OPP* values for various rf power densities. The decrease of carrier concentrations with increasing *OPP* is in agreement with the increase in film resistance with increasing *OPP* (see figure 7) according to the relation $R \propto 1/n$.

The decrease of electrical resistance R with increasing rf power density at *OPP* = 3% along with the simultaneous decrease of charge density n can be explained only by a stronger increase of carrier mobility that overweighs the decrease in charge density.

4. Conclusions

The dependence on *OPP* of structural, electrical and optical properties of AZO rf-magnetron-sputtered thin films, prepared at room temperature and low pressure of $p = 0.5$ mTorr, was studied at different rf power density values. The addition of oxygen to the Ar sputtering gas caused a deterioration of film crystallinity, a general increase in film electrical resistance and a change in the dependence of some film properties on rf power density. This was related to the high energy bombardment of negative oxygen ions during AZO film formation.

At low rf power density $P = 0.57$ W cm^{-2} the d-spacing increased with increasing *OPP*; however, it decreased with increasing *OPP* at high rf power density $P = 2.83$ W cm^{-2}. This result is related to the increase of interstitial atoms caused by the negative oxygen ion bombardment at low rf power density and with the formation of a more stoichiometric ZnO and Al_2O_3 at the grain boundaries of ZnO crystallites at high rf power density.

While electrical resistance increased with increasing rf power density at *OPP* = 0%, it decreased with increasing rf power density at *OPP* 3% and showed very high values with no monotonic dependence on rf power density at *OPP* 6%. While the increase of R when there was no oxygen addition has been related to the increase in the number of Al interstitial atoms with increasing rf power density, the decrease of R with increasing rf power density for *OPP* 3% is related to the formation of a more stoichiometric ZnO and the formation of Al_2O_3 at the grain boundaries of ZnO crystallites.

Optical transmission decreases with increasing *OPP* in the whole spectral range between 350 and 1000 nm. This can be related to the deteriorated film crystalline quality, which in turn leads to more optical scattering and absorption. Optical band gap, as well as carrier concentration, decreases with increasing rf power density or *OPP*.

References

[1] Flickyngerova S, Tvarozek V and Gaspierik P 2010 *J. Electr. Eng.* **61** 291
[2] Kim D, Yun I and Kim H 2010 *Curr. Appl. Phys.* **10** 459
[3] Granqvist C G 2007 *Sol. Energy Mater. Sol. Cells* **91** 1529
[4] Ali A I, Kim C H, Cho J H and Kim B G 2006 *J. Korean Phys. Soc.* **49** 652
[5] Yamamoto T and Katayama-Yoshida H 1999 *Jpn. J. Appl. Phys.* **38** L166
[6] Igasaki Y and Saito H 1991 *J. Appl. Phys.* **69** 2190
[7] Kim S S and Lee B T 2004 *Thin Solid Films* **446** 307
[8] Shan F K, Liu G X, Kim B I, Shin B C, Kim S C and Yu Y S 2003 *J. Korean Phys. Soc.* **42** 1157
[9] Sakai K, Kakeno T, Ikari T, Shirakata S, Sakemi T, Awai K *et al* 2006 *J. Appl. Phys.* **99** 043508
[10] Giancaterina S, Ben Amor S, Bachari E M, Baud G, Jacquet M and Perrin C 2001 *Surf. Coat. Technol.* **138** 84
[11] Ellmer K and Mientus R 2008 *Thin Solid Films* **516** 4620
[12] Fumagalli F, Martí-Rujas J and Di Fonzo F 2014 *Thin Solid Films* **569** 44
[13] Saad M and Kassis A 2012 *Mater. Chem. Phys.* **136** 205
[14] Chen J, Sun Y, Lv X, Li D, Fang L, Wang H *et al* 2014 *Appl. Surf. Sci.* **317** 1000
[15] Song D 2008 *Appl. Surf. Sci.* **254** 4171
[16] Zhou B, Rogachev A V, Liu Z, Piliptsou D G, Ji H and Jiang X 2012 *Appl. Surf. Sci.* **258** 5759
[17] Lee Y E, Lee J B, Kim Y J, Yang H K, Park J C and Kim H J 1996 *J. Vac. Sci. Technol. A* **14** 1943
[18] Bachari E M, Ben Amor S, Baud G and Jacquet M 2001 *Mater. Sci. Eng. B* **79** 165
[19] Bachari E M, Baud G, Ben Amor S and Jacquet M 1999 *Thin Solid Films* **348** 165
[20] Kamada Y, Furuta M, Hiramatsu T, Kawaharamura T, Wang D, Shimakawa S *et al* 2011 *Appl. Surf. Sci.* **258** 695
[21] Ellmer K, Cebulla R and Wendt R 1998 *Thin Solid Films* **317** 413
[22] Scherrer P 1918 *Göttinger Nachr.* **2** 98
[23] Nefedov V I, Firsov M N and Shaplygin I S 1982 *J. Electron Spectrosc. Relat. Phenom.* **26** 65
[24] Kim Y H, Lee K S, Lee T S, Cheong B, Seong T-Y and Kim W M 2009 *Appl. Surf. Sci.* **255** 7251
[25] Islam M N, Ghosh T B, Chopra K L and Acharya H N 1996 *Thin Solid Films* **280** 20
[26] Wang F H, Chang H P, Tseng C C and Huang C C 2011 *Surf. Coat. Technol.* **205** 5269
[27] Chen M, Wang X, Yu Y H, Pei Z L, Bai X D, Sun C *et al* 2000 *Appl. Surf. Sci.* **158** 134
[28] Zhu H, Bunte E, Hüpkes J, Siekmann H and Huang S M 2009 *Thin Solid Films* **517** 3161
[29] Yu X, Ma J, Ji F, Wang Y, Zhang X, Cheng C *et al* 2005 *J. Cryst. Growth* **274** 474
[30] Song D, Widenborg P, Chin W and Aberle A G 2002 *Sol. Energy Mater. Sol. Cells* **73** 1
[31] Kwak D J, Park M W and Sung Y M 2009 *Vacuum* **83** 113
[32] Morita A, Watanabem I and Shirai H 2011 *Thin Solid Films* **519** 6903
[33] Minami T, Sato H, Takata S, Ogawa N and Mouri T 1992 *Jpn. J. Appl. Phys.* **31** L1106
[34] Hou Q, Meng F and Sun J 2013 *Nanoscale Res. Lett.* **8** 144
[35] Yoshioka S, Oba F, Huang R, Tanaka I, Mizoguchi T and Yamamoto T 2008 *J. Appl. Phys.* **103** 014309
[36] Lany S and Zunger A 2007 *Phys. Rev. Lett.* **98** 045501
[37] Tauc J, Grigorovici R and Vancu A 1966 *Phys. Status Solidi B* **15** 627
[38] Özgür Ü, Alivov Y I, Liu C, Teke A, Reshchikov M A, Dogan S *et al* 2005 *J. Appl. Phys.* **98** 1
[39] Burstein E 1954 *Phys. Rev.* **93** 632
[40] Moss T S 1954 *Proc. R Soc. Lond. Ser. B* **67** 775
[41] Urbach F 1953 *Phys. Rev.* **92** 1324
[42] Sze S M 1981 *Physics of semiconductor devices* 2nd edn (New York: John Wiley & Sons) p 849